

15076 PORPHYRITIC SUBOPHITIC QUARTZ-NORMATIVE ST. 1 400.5 g
MARE BASALT

INTRODUCTION: 15076 is tough, coarse-grained basalt (Fig. 1) with some pigeonite phenocrysts. It has been dated as close to 3.35 b.y. old. The sample is blocky and angular, with a few planar fractures. It is light olive gray with a few irregularly distributed rugs containing plagioclase crystals. Its surface has some slickensides on one face, and a few zap pits occur on two sides. It had a small fillet when collected.

15076 was collected on the east flank of Elbow Crater, as one of five basalt samples collected on a line extending out from the crater (see Fig. 15065-1). 15076 was collected with 15075 and soil samples, about 25 m east of the Elbow Crater rim crest, as one of a cluster of rocks, all of which had the same surface texture and albedo.



Figure 1. Pre-split view of 15076. S-71-47769

PETROLOGY: 15076 is a coarse, quartz-normative mare basalt, lacking magnesian olivine but containing pigeonite phenocrysts (Fig. 2). The texture is essentially porphyritic and subophitic with very little interstitial glass, and the pigeonite phenocrysts are twinned and zoned. Tridymite is conspicuous in thin sections. Rhodes and Hubbard (1973) reported a mode of 66.3% pyroxene, 28.5% plagioclase, 0.5% ilmenite, 1.4% ulvospinel, 2.1% cristobalite, 0.5% troilite, 0.6% mesostasis, and traces of Cr-spinel and Fe-metal. They apparently identified tridymite as cristobalite. The PET report for thin section 12 (Lunar Sample Information Catalog Apollo 15, 1972) listed 55% clinopyroxene, 45% plagioclase, 2% tridymite, 2% ilmenite, 1% ulvospinel, and less than 0.1% each of Cr-spinel, troilite, and Fe-Ni metal. Brown et al. (1972a) reported 53% clinopyroxene and 36% plagioclase and noted the discrepancy with the PET report. The differences result from the coarse grain size and the small thin section size (less than 1 cm²). Peckett et al. (1972) noted the presence of tranquillityite as an accessory phase. Macroscopically the mafic silicates are yellowish green and zoned to brown, or are honey brown to red brown, and include about 10% subhedral prisms. The plagioclases are white to translucent and are dominantly laths. The low density (2.4 g/cm³) reported by O'Kelley et al. (1972) might reflect the vuggy nature of the sample analyzed.

The pyroxenes are mostly zoned, pigeonite to augite, and many are twinned. Most grains are not particularly elongated, but some are long, narrow, zoned phenocrysts (Fig. 2c,d). Microprobe analyses of pyroxenes were reported by Brown et al. (1972a,b), and by Virgo (1972, 1973). These data are very similar (Fig. 3) and show heterogeneous zoning from pigeonite to subcalcic ferroaugite, or to subcalcic augite and then rapid zoning over narrow rims to subcalcic ferroaugite. One crystal showed oscillatory zoning of subcalcic augite (Virgo, 1972). The Ti/Al ratio starts at 1/6, and stays constant until subcalcic augite is reached, and then rapidly increases to 1/2 (Virgo, 1972) (Fig. 4), an abrupt change attributed to the start of plagioclase crystallization. Possibly Ti³⁺ is present. Brown et al. (1972b) diagrammed similar Ti/Al variations, but did not distinguish data for 15076 from data for 15085 and 15555. Papanastassiou and Wasserburg (1972) listed a pyroxferroite analysis (45% FeO, 47% SiO₂, 6% CaO, 1.8% MgO). Virgo (1972, 1973) used Mossbauer spectroscopy to provide information on the Fe²⁺, Mg distribution, tabulating site occupancies, and calculated distribution coefficients. The site occupancies suggest a temperature of 560°C (Virgo, 1972) or 580°C (Virgo, 1973), significantly below the critical temperature for ordering (500°C-810°C), indicating slow cooling below the critical temperature. There is no evidence for Fe³⁺. Virgo (1972) also reported x-ray diffraction data, showing diffuse streaking for pigeonite reflection along both a* and c*, which point toward the expected position of the augite reflections and hence indicate very fine-scale exsolution. Jagodzinski and Korekawa (1973) also found diffuse x-ray scattering resulting from the exsolution process, even though no reflections of the exsolved augite or pigeonite itself could be seen. In the same study, Berking et al. (1972) reported x-ray diffraction results for pigeonites, and found four to have the space group P2₁/c, and tabulated the lattice parameters, which indicate a low-Ca pyroxene. The other sample is different. Fernandez-Moran et al. (1973) studied homogeneous pigeonites using electron optical techniques, and showed electron micrographs and electron diffraction patterns. They observed exsolution in 32% of their samples, with a lamella structure with band widths of 100 to 1800 Å (average 1000 Å) and interband widths of 300 to 6200 Å (average 3100 Å).



Fig. 2a



Fig. 2b

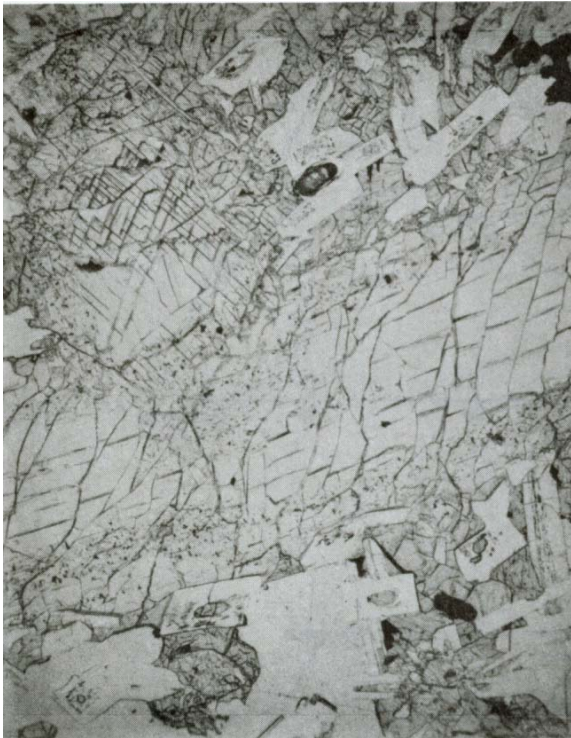


Fig. 2c



Fig. 2d



Fig. 2e

Figure 2. Photomicrographs of 15076. Widths about 3 mm.
a)c) transmitted light; b)d)e) crossed polarizers, a)-d)15076,71; e) 15076,17.
a)b) general groundmass view showing cored, stubby, lathy plagioclases,
c)d) portion of a 1 cm long pigeonite phenocryst, and twinned pigeonite cross section,
e) small tridymite laths at common extinction.

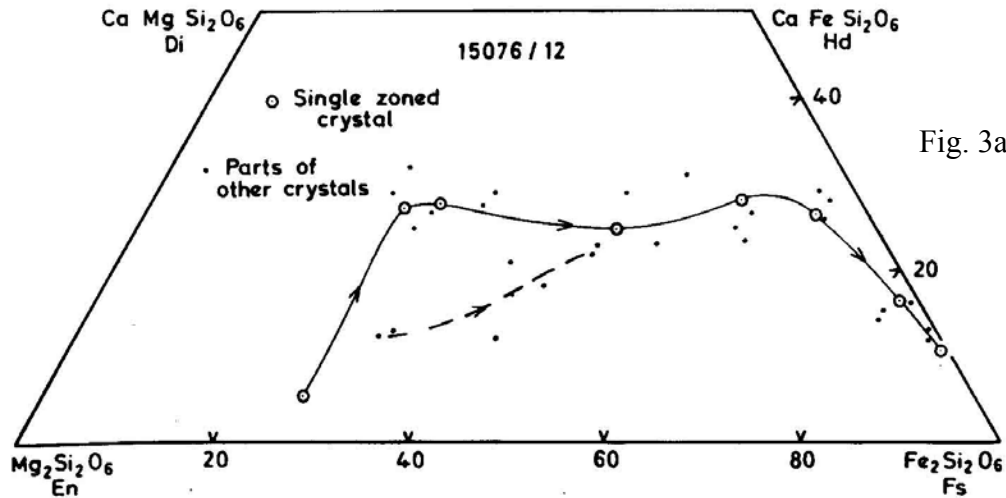


Fig. 3a

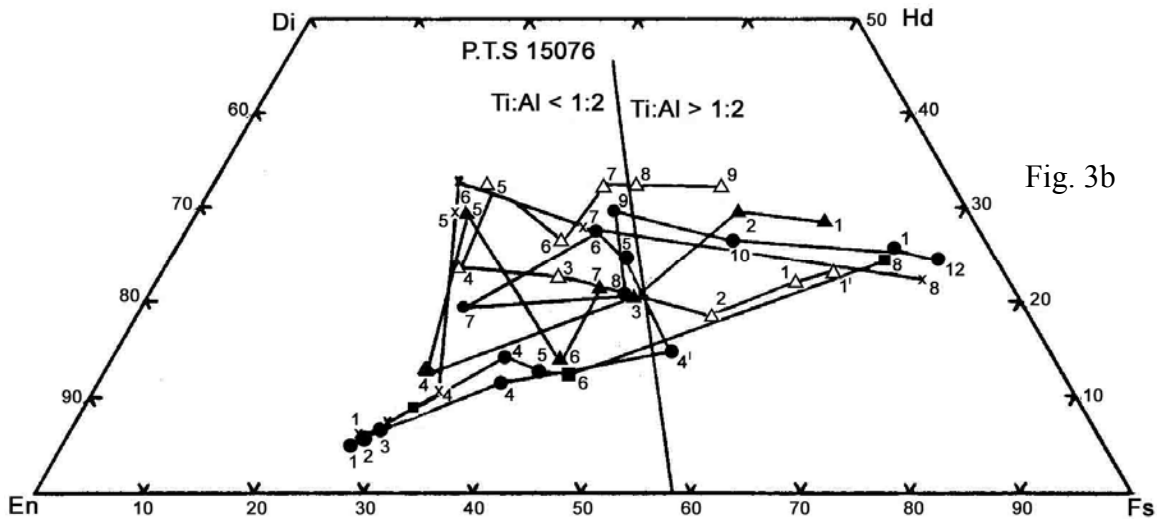


Fig. 3b

Figure 3. Compositions of pyroxenes on pyroxene quadrilateral
 a) Brown et al. (1972b). b) Virgo (1972).

Feldspars are dominantly lathy or prismatic, and some are hollow. Many contain a well-defined core-zone consisting of pyroxene and plagioclase. This core is commonly rectangular (Fig. 2b,c), and sharply bounded. Brown et al. (1972b) reported oscillatory zoning ($An_{89-82-89-72}$), but little chemical data for the plagioclases has been reported. Berking et al. (1972), Jagodzinski and Korekawa (1973), and Korekawa and Jagodzinski (1974) reported compositions of $An_{85 \pm 3}$ (optical determinations) for three plagioclases protruding into vugs. X-ray data show that two of these crystals are untwinned, the other twinned (albite and carlsbad). The patterns show reflections and diffusions whose possible causes are discussed in Berking et al. (1972) and Jagodzinski and Korekawa (1973). Two of the plagioclase crystals have peculiar mound-shaped surface features with pillars or whiskers on the surface.

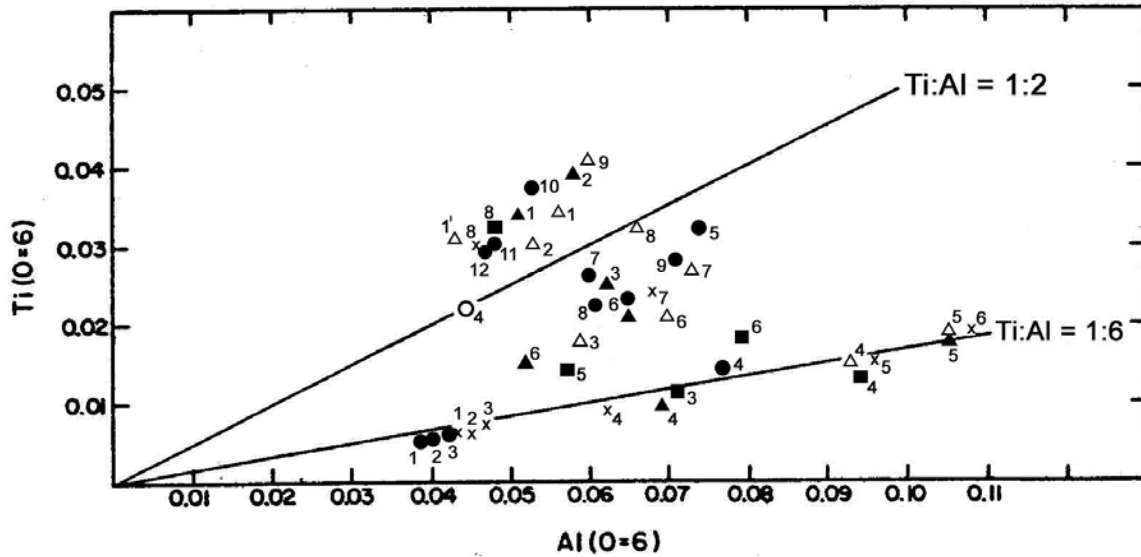


Figure 4. Ti vs. Al for pyroxenes (Virgo, 1972).

L. Taylor et al. (1975) plotted analyses of spinels (Fig. 5) and metals (Fig. 6). The sample is considered anomalous in that they observed no chromite, only ulvospinel, although this might be a sampling problem. The metal compositions show a substantial range compared with other coarse quartz-normative mare basalts. Jagodzinski and Korekawa (1973) showed Weissenberg photographs of tridymite, which has subcell dimensions like terrestrial high tridymite. The photographs also show additional reflections, some of which are strong, others diffuse. Brown et al. (1972b) listed an analysis of a rhyolitic residuum.

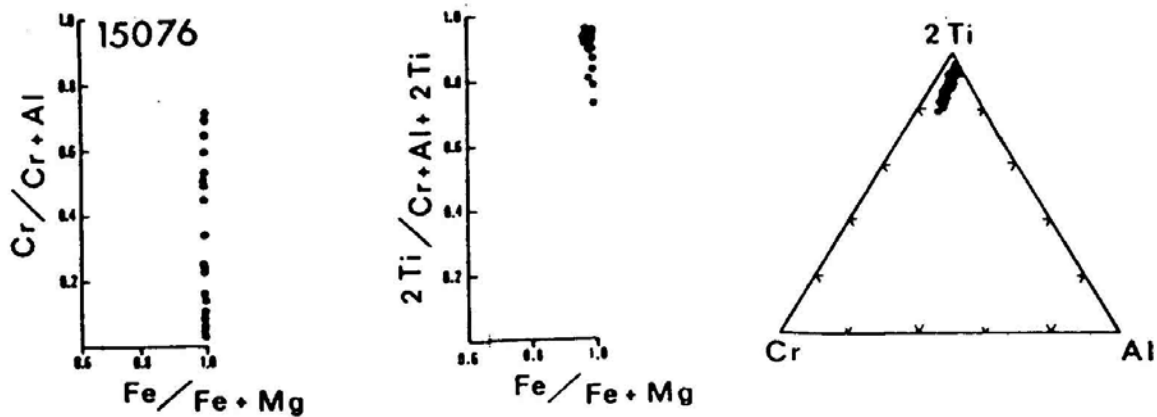


Figure 5. Compositions of spinels (L. Taylor et al., 1975).

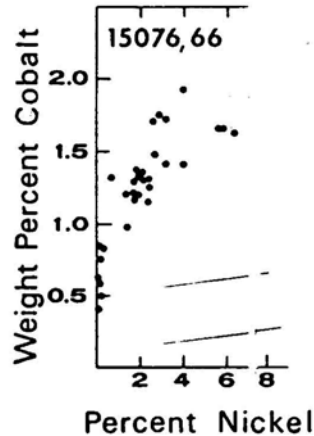


Figure 6. Compositions of metals
(L. Taylor et al., 1975).

Cooling Rates: In a series of papers, L. Taylor used the Zr partitioning between ilmenite and ulvospinel to determine cooling rates for 15076 (Taylor and McCallister 1972a,b; L. Taylor et al., 1973, 1975b; Onorato et al., 1979). Early data was reported erroneously, and L. Taylor et al. (1975) reported the correct data, with Zr ilmenite/Zr ulvospinel ratios of 1½ to 2 (1.88 average), which, by comparison with their experimental data, is consistent with an equilibration temperature of 949°C and a cooling rate of 6°C/day (corrected from L. Taylor et al., 1975a, value of 95°C/day). The underlying solute partitioning model was further improved by Onorato et al. (1979) and, following experiments to find the Zr diffusion coefficient, a cooling rate of 0.6°C to 2.1°C/day was derived. A grain size function calculated in provided a variation from 2.1°C to 3.2°C/day.

Lofgren et al. (1975), using a comparison of phenocryst morphologies and rock textures with those produced in dynamic crystallization experiments (known linear cooling rates), determined that both the phenocrysts and the matrix crystallized during cooling at less than 1°C/hr. Grove and Walker (1977), in a similar but more refined study, also determined cooling rates. From the pyroxene nucleation density they determined a rate of about 0.1°C/hr for early stage cooling, and from plagioclase dimensions determined a rate of about 0.2°C/hr for the late stage cooling. They suggested that the final position from a conductive boundary was 263 cm; Brett (1975), on the basis of then-available and limited kinetic data, had suggested that 15076 cooled in a flow about 1 m thick.

EXPERIMENTAL PEROLOGY: Humphries et al. (1972) diagrammed the results of equilibrium crystallization experiments on 15076, at an fO_2 of Fe/FeO equilibrium. The sequence is spinel at about 1230°C, ol + pig + spinel at about 1190°C (ol out by 1180°C), then sp + pig + oxide to 1150°C where plagioclase enters and spinel goes out. Clinopyroxene enters at about 1120°C and by then the charge is almost solid. As they do for other mare basalts, they believe the mafic nature of the rock is from mafic mineral accumulation, hence that the liquid was erupted at 1150°C at an ol-pig-plag cotectic. Most authors disagree with such an interpretation. Grove and Lindsley (1979) used the

composition of 15076 in their study to determine pigeonite-liquid partition coefficients for Fe, Mg, Ca, Cr, Al, Ti, and Mn.

All other experimental work has been dynamic, referred to under "Cooling Rates," above.

CHEMISTRY: Chemical analyses for bulk rock are listed in Table 1, and rare earths are plotted in Figure 7. The data are not entirely consistent (e.g., variation in TiO₂, MgO), presumably a consequence of small sample size and coarse grain size. The data clearly show 15076 to be one of the quartz-normative mare basalts.

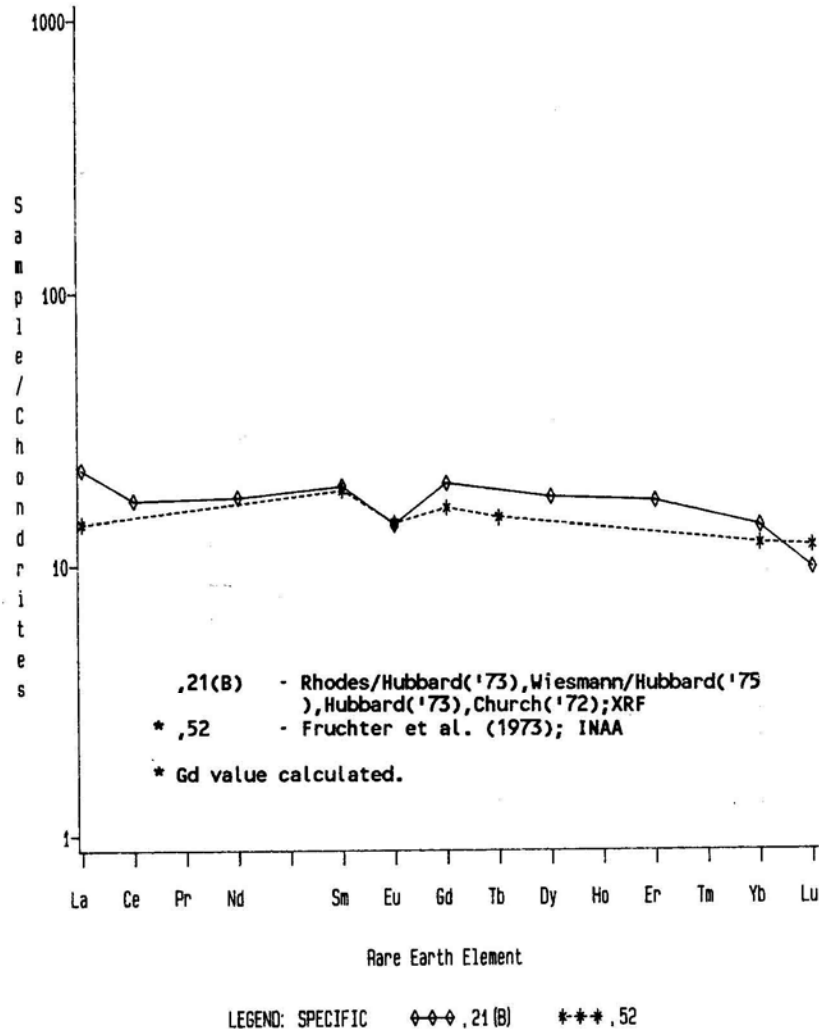


Figure 7. Rare earths in 15076.

The averages would indicate that 15076 is a rather average Apollo 15 quartz-normative basalt. Hubbard and Rhodes (1973) noted that agreement between their two splits was poor. Rhodes (1972) used the composition in producing an average for the quartz-normative basalts, Christian et al. (1972) and Cuttitta et al. (1973) also reported an

TABLE 15076-1. Chemical analyses of 15076

	,24	,2	,21	,21	,21	,52	?	,0	,23	,3	,10	?	,20
Wt % SiO2	48.82	48.80	48.06										
TiO2	1.83	1.46	2.01	1.90		1.47							
Al2O3	8.31	9.30	9.63			9.26							
FeO	20.45	18.62	20.22	18.5		19.74							
MgO	9.43	9.46	7.80	7.75									
CaO	10.30	10.82	10.74								10.6		
Na2O	0.40	0.26	0.29	0.30		0.30							
K2O	0.08	0.03	0.05	0.049				0.049			0.044		
P2O5	0.05	0.03	0.08										
(ppm) Sc	40					47							
V	135												
Cr	2123					3380							
Mn	2250	2090	2250										
Co	42					41							
Ni	32		11										
Rb	1.2		1.1	0.917	0.924								
Sr	98		120	112	111.8								
Y	26		29										
Zr	64		97										
Nb	<10		6.2										
Hf						2.1							2.866
Ba	58			62.7									
Th							0.5901	0.45					
U				0.149			0.1532	0.12					
Pb							0.266						
La	10			7.38		4.7							
Ce				15.1									
Pr													
Nd				10.6									11.850
Sm				3.52		3.4							3.796
Eu				0.970		0.98							
Gd				4.95									
Tb						0.7							
Dy				5.60									
Ho													
Er				3.40									
Tm													
Yb	3.7			2.77		2.4							
Lu				0.326		0.40							0.394
Li	5.6												
Be	1.2												
B										21			
C													
N													
S		300	800						452/499		970		
F													
Cl													
Br													
Cu	9.1												
Zn													
(ppb) I													
At													
Ga	4100												
Ge													
As													
Se													
Mo													
Tc													
Ru													
Rh													
Pd													
Ag													
Cd													
In													
Sn													
Sb													
Te													
Cs													
Ta					440								
W													
Re													
Os													
Ir													
Pt													
Au													
Hg													
Tl													
Bi													
	(1)	(2)	(2)	(2)	(3)	(4)	(5)	(6)	(7)	(8)	(9)	(10)	(11)

References to Table 15076-1

References and methods:

- (1) Christian et al. (1972), Cottitta et al. (1973); XRF, semi-micro chemical, optical emission spec.
- (2) Rhodes and Hubbard (1973), Wiesmann and Hubbard (1975), Hubbard et al. (1973), Church et al. (1972); XRF, ID/MS
- (3) Nyquist et al. (1972, 1973); ID/MS
- (4) Fruchter et al. (1973); INAA
- (5) Tatsumoto et al. (1972); ID/MS
- (6) O'Kelley et al. (1972); gamma ray spec.
- (7) Thode and Rees (1972);
- (8) Moore et al. (1972, 1973); combustion, GC
- (9) Stettler et al. (1973); Ar-isotopes, irradiation
- (10) Gibson et al. (1975); combustion
- (11) Unruh et al. (1983); ID/MS

“excess reducing capacity” of +0.18, and analyzed for but found no Fe₂O₃. Light element abundances are similar to those for other mare basalts; the S analyses show a wide variation, and those data from combustion (e.g., Gibson et al., 1975, 970 ppm) are probably more reliable and reasonable than those from acid hydrolysis, etc. Gibson et al. (1975) also analyzed for C in CO (3.0 ppm C), in CO₂ (10.6 ppm C), for H in H₂ (18.6 ppm H) for S in H₂S (651 ppm S), and for Fe⁰ (1040 ppm by hydrolysis, 940 by magnetism).

STABLE ISOTOPES: Sulfur isotopic analyses were reported by Thode and Rees (1972) ($\lambda^{34}\text{S} \text{ ‰} = 0.57$) and Gibson et al. (1975) ($\lambda^{34}\text{S} \text{ ‰} = -1.2$). These isotopic values are similar to those of other mare basalts.

RADIOGENIC ISOTOPES AND GEOCHRONOLOGY: Papanastassiou and Wasserburg (1973) reported a Rb-Sr internal isochron age of 3.33 ± 0.08 b.y. with initial $^{87}\text{Sr}/^{86}\text{Sr}$ of 0.69927 ± 8 , within error the same as other Apollo 15 mare basalts. The isochron is based on tabulated data for plagioclase, “ilmenite”, and “cristobalite” separates. Nyquist et al. (1972, 1973) and Wiesmann and Hubbard (1975) reported whole rock $^{87}\text{Rb}/^{86}\text{Sr}$ of 0.0237 ± 4 and $^{87}\text{Sr}/^{86}\text{Sr}$ of 0.70051 ± 7 , consistent with the internal isochron when an appropriate interlaboratory correction is made.

Stettler et al. (1973) reported a $^{40}\text{Ar}-^{39}\text{Ar}$ high temperature plateau age of 3.35 ± 0.04 b.y. (Fig. 8). The Ca/K release is similar to other mare basalts and demonstrates that K is not located in a single phase. Kirsten et al. (1973) reported a $^{40}\text{Ar}-^{39}\text{Ar}$ plateau age which is the same, 3.35 ± 0.15 b.y.

Tatsumoto et al. (1972) reported U, Th, and Pb isotopic data for a whole-rock sample (Table 2). The data lies, with 15065, 15085, and 15476, on a 3.5 to 4.65 b.y. model discordia line. Rosholt and Tatsumoto (1973) and Rosholt (1974) discussed α -spectrometry measurements of $^{232}\text{Th}/^{230}\text{Th}$ as compared with the value for that ratio expected from the $^{232}\text{Th}/^{238}\text{U}$ concentration ratio. The expected/measured ratio of 1.48 was the highest among A15 mare basalts, and Rosholt (1974) discussed possible and probable reasons for the discrepancy.

Unruh et al. (1984) reported Sm-Nd and Lu-Hf whole rock isotopic data (Table 3). The Sm/Nd, Lu/Hf, ϵ Nd, and ϵ Hf values are similar to those for other Apollo 15 mare

basalts, which are discussed as a group. 15076 underwent Sm/Nd and Lu/Hf fractionations at the time of melting, 3.3 b.y. ago.

RARE GASES, COSMOGENIC NUCLIDES, TRACKS, MICROCRATERS, AND EXPOSURE: Stettler et al. (1973) and Kirsten et al. (1973) reported ^{38}Ar exposure ages of 330 m.y. and 280 m.y. respectively. This age is similar to that obtained by the same method for 15075, but much older than the track and microcrater ages (below).

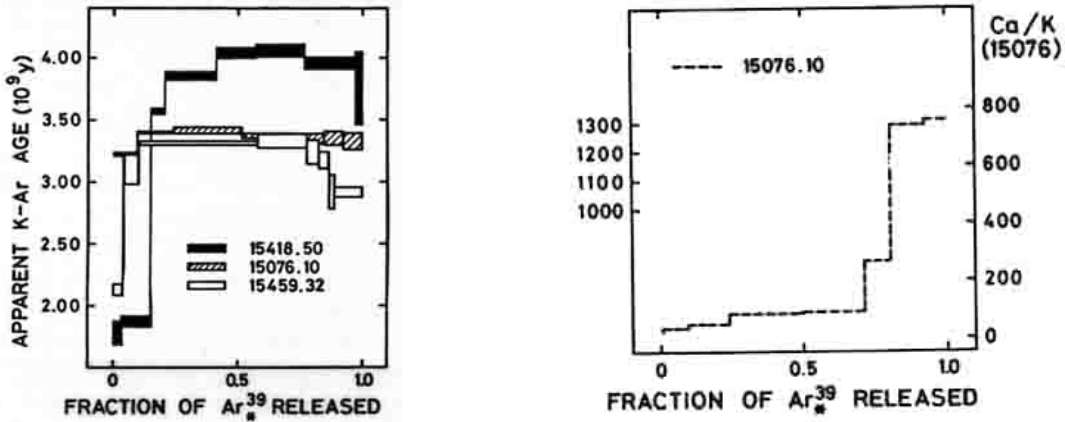


Figure 8. Ar release and Ca/K release for 15076,10 (Stettler et al., 1973).

TABLE 15076-2. U, Th, Pb isotopic data (Tatsumoto et al., 1972).

$^{206}\text{Pb}/^{204}\text{Pb}$	$^{207}\text{Pb}/^{204}\text{Pb}$	$^{208}\text{Pb}/^{204}\text{Pb}$	$^{232}\text{Th}/^{238}\text{U}$	$^{238}\text{U}/^{204}\text{Pb}$
374.4	155.8	393.1	3.98	460

Corrected for analytical blanks.

TABLE 15076-3. Sm/Nd and Lu/Nf whole-rock data for 15076,20 (Unruh et al., 1984)

$\frac{^{147}\text{Sm}}{^{144}\text{Nd}}$	$\frac{^{143}\text{Nd}}{^{144}\text{Nd}}$ \circ ϵ_{Nd} \circ	$\frac{^{143}\text{Nd}}{^{144}\text{Nd}}$ I ϵ_{Nd} I	$\frac{^{176}\text{Lu}}{^{177}\text{Hf}}$	$\frac{^{176}\text{Hf}}{^{177}\text{Hf}}$ \circ ϵ_{Hf} \circ	$\frac{^{176}\text{Hf}}{^{177}\text{Hf}}$ I ϵ_{Hf} I
0.1936 ± 2	0.512700 ± 16 ± 0.3	0.50854 ± 2 ± 0.4	0.01949 ± 3	0.282344 ± 67 -18.3 ± 2.4	0.28108 ± 7 $+13.8$ ± 2.5

\circ = at present day; I = at time of crystallization

Eldridge et al. (1972) reported cosmogenic nuclide disintegration count data for ^{22}Na , ^{26}Al , ^{46}Sc , and ^{54}Mn . They noted that the ^{22}Na appeared to have reached equilibrium, even though the chemistry was not known, but ^{26}Al was marginal; they suggested an

exposure age of at least 2 m.y. Yokoyama et al. (1974) normalized the data for chemical composition, but were still unable to decide if the ^{26}Al activity was saturated or not.

Solar flare track density/depth relationships were studied by the Heidelberg group (Schneider et al., 1972, 1973a,b; Storzer et al., 1973; Fechtig et al., 1974). Their track density/depth measurements are summarized in Figure 9, with other samples for comparison. The original age determined, 8.5×10^4 years, was revised up to 2.6×10^5 years (Fechtig et al., 1974) or 2.8×10^5 years (Horz et al., 1975) using a new flux calibration. This track age is significantly lower than the ^{38}Ar age, suggesting a recent exposure from a shallow depth of burial. Kratschmer and Gentner (1975) used a method for identifying heavy ions from their etchable tracks in feldspars, applying the results to fossil cosmic-ray and Fe calibration tracks to obtain information about the nuclear composition of the ancient cosmic radiation. The distributions of the track etching rates and the residual ranges for both fossil and calibration tracks were compared, but a definitive interpretation was not possible because the influence of annealing and the crystallographic effects were insufficiently known.

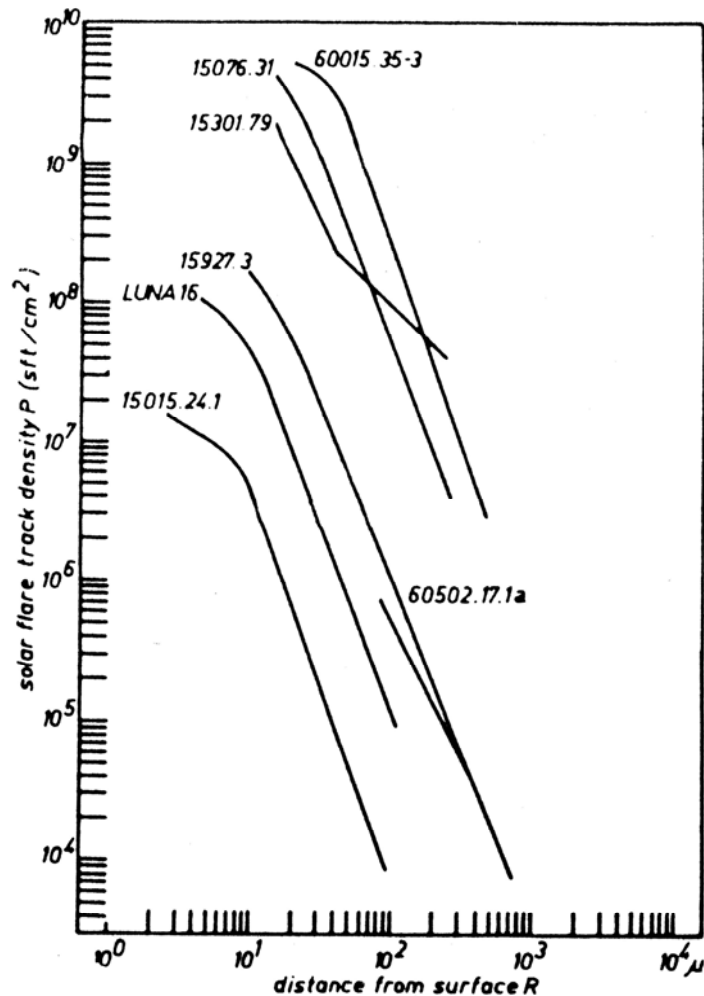


Figure 9. Depth dependence of solar flare tracks on 15076,31 and other samples (Storzer et al., 1973).

Microcraters were studied by Schneider et al. (1973b) (0.1 to 10 microns) and by Morrison et al. (1973) (100 to 1,000 microns). Cumulative frequency/diameter diagrams are shown as Figure 10 and 11. Schneider et al. (1973b) used an SEM and noted that their statistics were good in the less than 1 micron range, but poor above this size. They estimated a cosmic dust flux in the submicron range from the size distribution and exposure age (solar flare) (Fig. 12); this flux was lower than that from satellite-borne detectors (the later change in the solar flare calibration to make the exposure older would decrease the calculated flux). Brownlee et al. (1972) noted that the crater density was very low, about 10 times less than 15286 or Luna 16 glass. Morrison et al. (1973) also found an exceptionally low frequency of craters, and estimated the age as 8 to 17×10^5 years. Combined with the Schneider et al. (1973b) data, there appears to be a flexure in the distribution below 100 microns and probably at about 10 microns if both surfaces investigated are actually the same age.

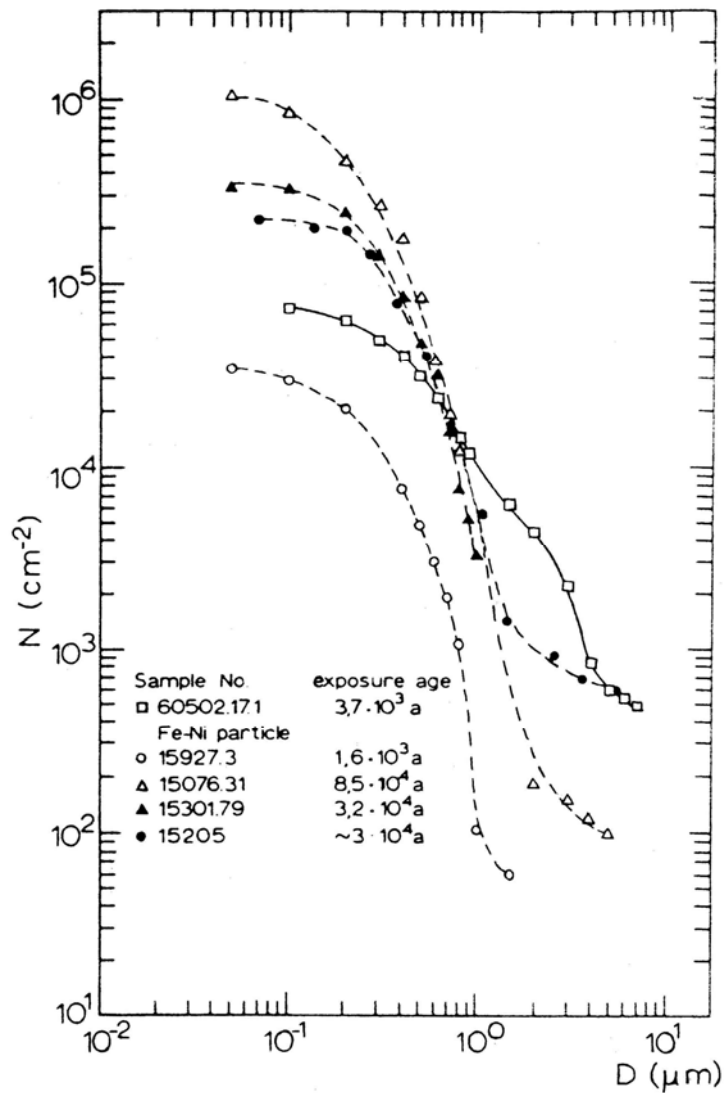


Figure 10. Cumulative crater densities N vs. pit diameter D for 15076 and other samples (Schneider et al., 1973b).

PHYSICAL PROPERTIES: Gose et al. (1972) and Pearce et al. (1973) reported magnetic data (Table 4), including NRM in some detail. The NRM is similar to other basalts (between 10^{-5} and 10^{-6} emu/g). Under AF-demagnetization, two chips had stable magnetization (Fig. 13). A soft magnetization was eliminated after cleaning in 250 Oe, and there were no major changes in intensity or direction up to 150 Oe. However, Brecher (1975, 1976) listed 15076 under her category of rocks "inhomogeneous in NRM intensity or direction," presumably because of the higher stable intensity of ,50 (Fig. 13).

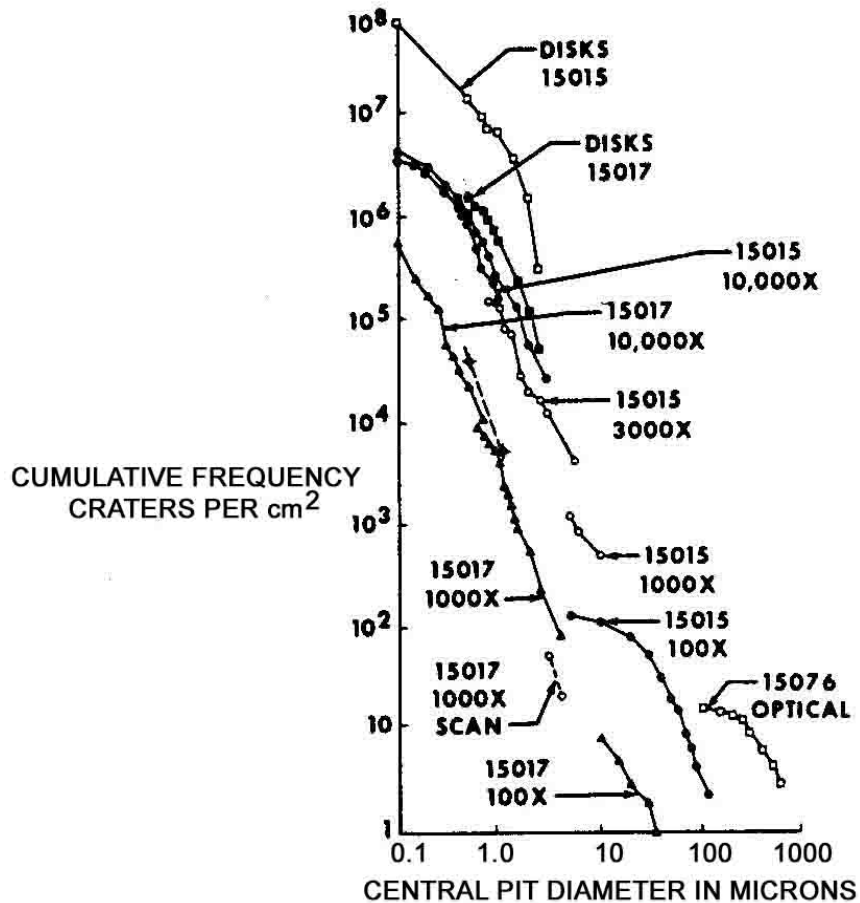


Figure 11. Cumulative crater density vs. pit diameter for 15076 and other samples (Morrison et al., 1973).

TABLE 15076-4. Room temperature magnetic data (Pearce et al., 1973)

J emu/g	X_p emu/g	Oe	X_o emu/g	Oe	J _{rs} /J _s	H _c Oe	J _s /X _o KOe	Equiv Fe ^o	Equiv. Fe ²¹
0.21	33.8		0.53		0.004	11.0	3.9	0.095	15.5

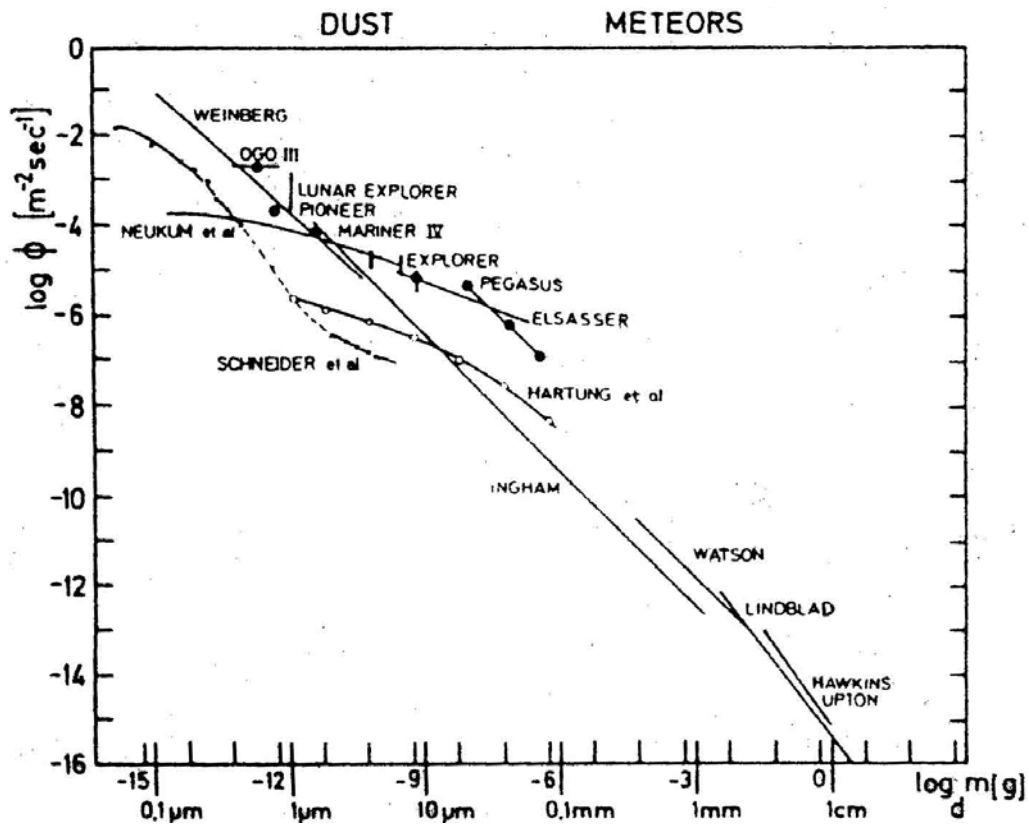


Figure 12. Cumulative cosmic dust fluxes plotted against particle masses and diameters. Line marked "Schneider et al." is from 15076 data (Schneider et al., 1973b).

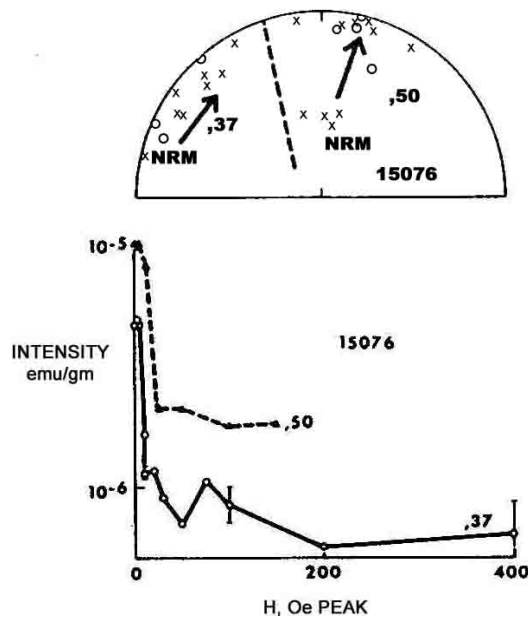


Figure 13. AF demagnetization of two splits of 15076. Arrows show change in direction upon demagnetization (Pearce et al., 1973).

PROCESSING AND SUBDIVISIONS: A chip was taken from ,0, and subsplit to make samples ,1 to ,11, some of which were interior only and some of which had exterior. ,4 was potted and produced thin sections ,12 and ,14 to ,19, and ,11 was subsplit (,20 to ,24) for isotopic and chemical analyses. Subsequently, the sample was sawn (1972) and a slab subdivided as shown in Figure 14. Several of these pieces were further subdivided, including ,28, which was potted and produced thin sections ,68 to ,72. In 1975 the "W" end was sawn off (Fig. 14) and subdivided (,87, 6.6 g; ,88, 44.4 g; ,89, 3.96 g; and ,90, 5.2 g) for remote storage at Brooks. ,0 now has a mass of 239.5 g. Nearly all other pieces are less than 4 g each.

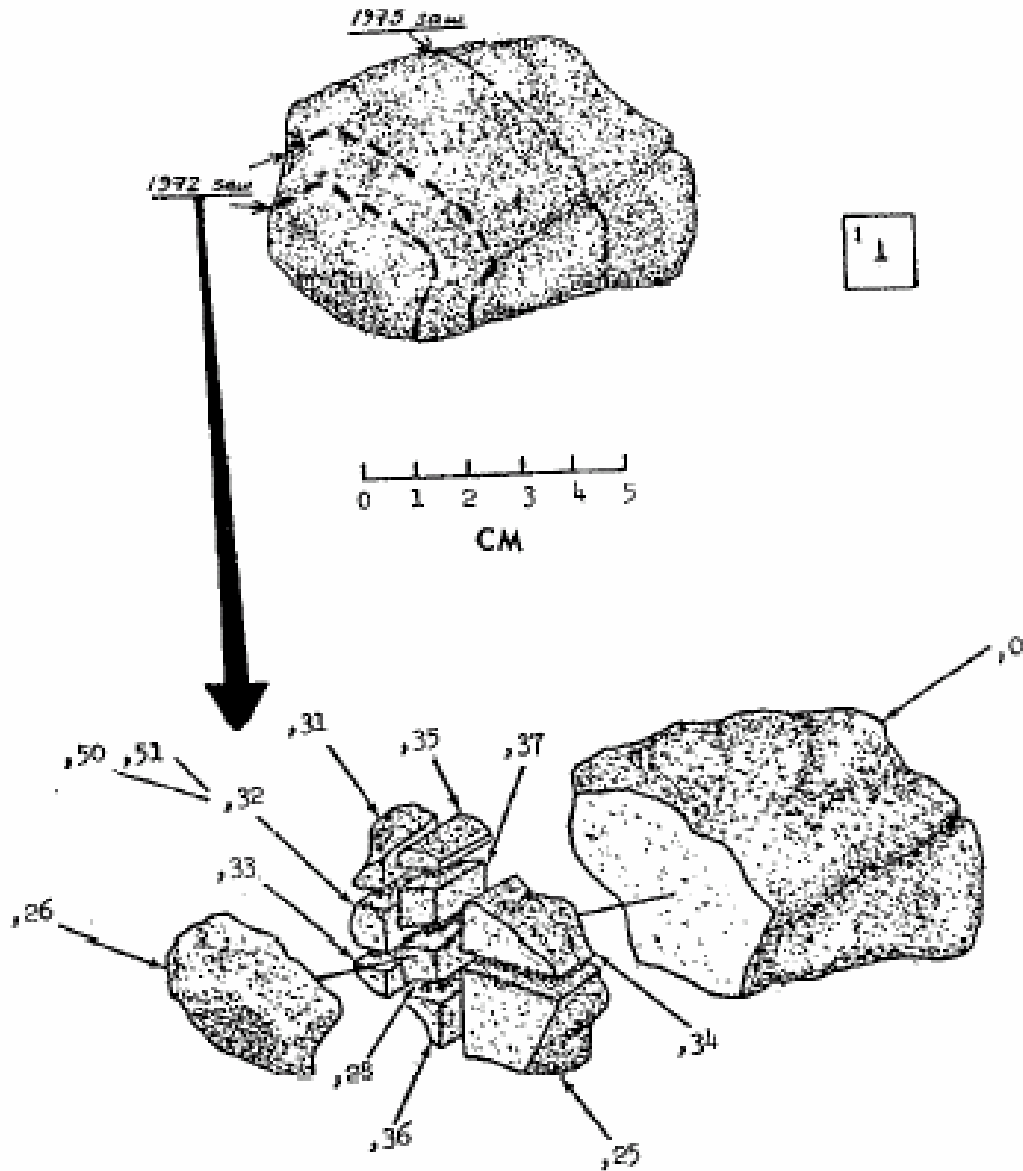


Figure 14. Sawing of 15076, in 1972 and 1975.